


Innovative applications of rotaxane-based molecular junctions in electronics and optoelectronics

Hiba Abbas Mohammed* , Oday A. Al-Owaedi ,
Hussein Neama Najeeb 

Department of Laser Physics, College of Science for Women, University of Babylon, Hilla, Iraq.

*Corresponding author: hibaabaas45@gmail.com

Original Research

Abstract:

Received:
22 June 2024
Revised:
20 July 2024
Accepted:
26 July 2024
Published online:
30 August 2024

© The Author(s) 2024

This study examines the effect of aromatic ring numbers on electronic and transport properties in rotaxane molecular junctions using density functional theory (DFT) calculations. Five rotaxane molecules (R-1 to R-5) with varying ring counts (1 to 5) and 149 (R-1) to 422 (R-5) atoms. Our results showed that the ring count significantly influenced properties like as band gap, fermi energy, binding energy and so on. The HOMO-LUMO gap decreased from -1.14 eV to -1.05 eV for R-1 and R-5 respectively which indicating improved conductivity. Electron transfer increased from 1.6×10^{-4} in R-1 structure to 2.3×10^{-3} in R-5 from transmission coefficient and the impact of ring count was consistent across different temperatures. Electrical conductance (G/G_0) followed a similar trend, increasing from 1.5×10^{-4} (R-1) to 2.2×10^{-3} (R-5) with Fermi energy. Threshold voltage (V_{th}) and seebeck coefficient (S) decreased with more rings in opposite manner and finally the Binding energy (B.E.) exhibited non-monotonic behavior. This study underscores the significant influence of aromatic ring count on electronic and transport properties in rotaxane molecular junctions, informing the design of molecular structures for drug delivery.

Keywords: Density functional theory; Transmission coefficient $T(E)$; Drug delivery

1. Introduction

The field of molecular electronics is based on exploiting molecules as fundamental units for computing and other electronic functions [1]. This gives molecular electronics an attractive role in the technology field because it provides the ultimate size for system scaling [2]. There have been numerous past efforts to develop this field which are focused on characterization, fabrication, and design of such devices. Today electronic devices reduced to sizes on the molecular scale are considered a major step to advances in modern technology [3]. The main challenge in this field is to find convenient molecular functions, materials and techniques to reach desirable properties for electronic devices. Rotaxane molecule is one possible candidate for molecular electronics, due to its unique properties which are particularly varied due to the unique characteristics of these molecules. A rotaxane is a mechanically interlocked molecular architecture consisting of a linear molecule (the axle) that is threaded through a macrocycle (the wheel) as

shown in Figure 1 [4]. The wheel and axle components are typically held together by non-covalent interactions, such as hydrogen bonding or coordination bonds. The structural and morphological features of a rotaxane molecule can vary depending on the specific design of the molecule [5]. However, in general, a rotaxane molecule can be described as having three main parts: the wheel, the axle, and the stoppers. The wheel is typically a cyclic molecule with a cavity that is large enough to accommodate the axle. The wheel can be made from a variety of cyclic compounds, such as crown ethers, Cyclodextrins, or Calixarenes. The size and shape of the wheel can be tailored to fit the specific properties of the axle. The axle is a linear molecule that is threaded through the cavity of the wheel [6]. The structural and morphological features of a rotaxane molecule are designed to create mechanically interlocked architecture that can exhibit unique properties, such as molecular switching or molecular machines. On the other hand, significant progress in experimental techniques, such as scanning

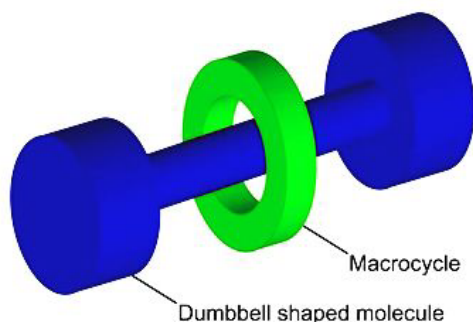


Figure 1. Graphical representation of a rotaxane.

tunneling microscopy STM [7], gives the ability to study the electronic single molecule properties through imaging, combined with measurement of the electronic response of the molecules. The main challenge in this field is to find convenient molecular functions, materials and techniques to reach desirable properties for electronic devices. This study envisage the morphological, structural, electrical and thermoelectric properties of rotaxane molecular junctions using density functional theory methods (DFT)[8, 9] and Quantum Transport Theory (QTT)[10].

2. Computational methods

Initially, the electronic structures of all molecules were computed at double- ζ polarized zeta DPZ basis set. Plots of the highest occupied and lowest unoccupied molecular orbitals (HOMO and LUMO, respectively) are shown in Figure 2. To elucidate the experimentally observed trends, and to better evaluate the transport properties of these molecular junctions, Calculations by using a combination of DFT (the SIESTA code) [11] and a non-equilibrium Green's function formalism were also carried out. This DFT-Landauer approach used in the modeling assumes that on the time scale taken by an electron to traverse the molecule, inelastic scattering is negligible. This is known to be an accurate assumption for molecules up to several nanometers in length. For the transport calculations, each molecule was attached to opposing 35-atom (111) directed pyramidal gold electrodes, then geometrical optimization was carried out by using the DFT code SIESTA, with a generalized gradient approximation [11, 12]. These layers were then further repeated to yield infinitely-long current-carrying gold electrodes. From these model junctions the transmission coefficient, $T(E)$, was calculated using the Gollum code [13]. The use of DFT to compute the ground state energy of various molecular junctions, allows binding energies and optimal geometries to be computed.

3. Results and discussion

3.1 Structural properties

The rotaxane molecules [14] are shown in Figures 2 and 3, which are identical in their backbone (the axle) and differ in the number of rings (macrocycle wheels). The number of rings has been increased from one ring for molecule R-1 to five rings for molecule R-5. The backbone of the rotaxane

molecules ends with an anchor groups called stoppers. The stoppers are bulky groups attached to the ends of the axle that prevent rings from slipping out of the wheel cavity. The stoppers consist of phenyl rings attached to the pyridine ring, which is the bonding ring of the molecule. The axle is composed of nine carbon-carbon triple bonds and nine of carbon-carbon single bonds, which result in an important property called the π -conjugated structure. The wheel is typically a cyclic molecule consisted of phenyl

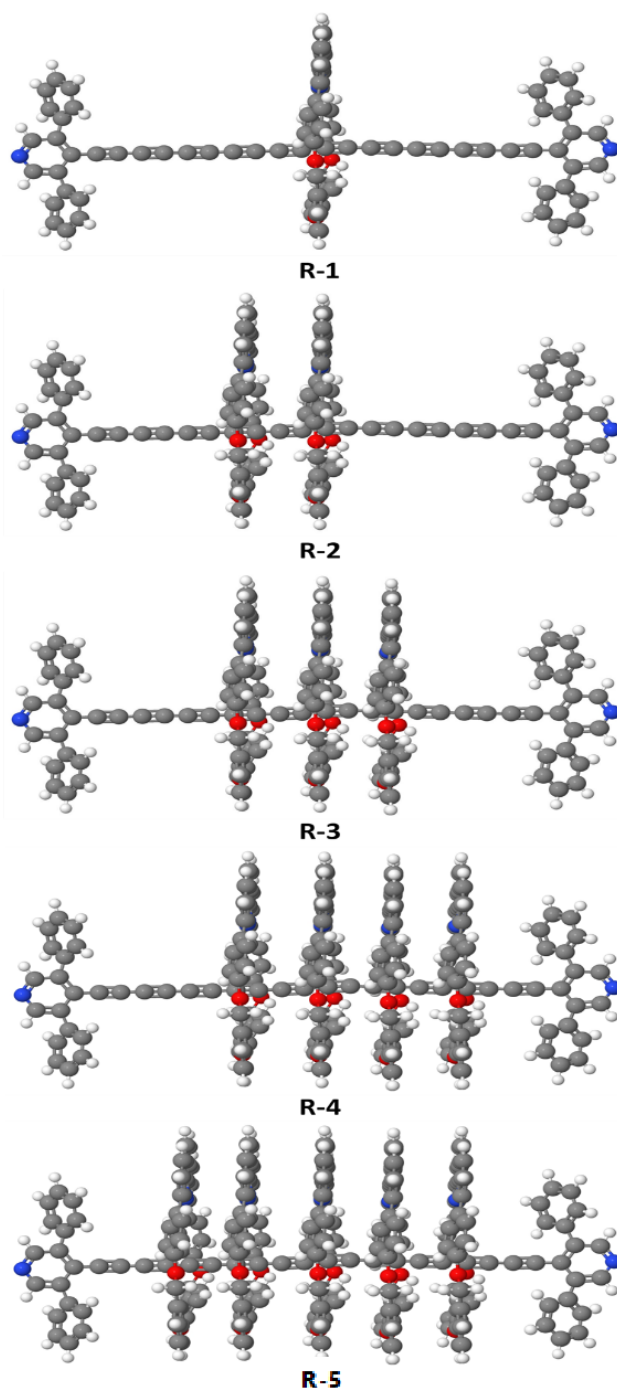


Figure 2. The optimized geometries at ground state of all molecules. The red balls are oxygen atoms, grey are carbon atoms, the white ones are hydrogen atoms, and the blue ones are nitrogen atoms.

rings linked to pyridine rings at the upper part, while the lower part consisted of phenyl rings combined with three oxygen atoms.

3.2 Electronic properties

3.2.1 Transmission coefficient $T(E)$

The electronic properties of rotaxanes can be influenced by the presence of the macrocycle and the axle, as well as the nature of their interactions [15]. The macrocycle in a rotaxane can act as an electron donor or acceptor, depending on its functional groups and the nature of its interactions with the axle [16].

The transmission coefficient $T(E)$ is a property of the whole system comprising the leads, the molecule and the contact between the leads and the molecule [17]. In general, the transmission coefficient $T(E)$ describing the propagation of electrons of energy E from the left to the right electrode. In this thesis, the transmission coefficient has been calculated by first obtaining the corresponding Hamiltonian and overlap matrices using SIESTA and then using the GOL-LUM code. Figure 4 shows that R-5 introduces a high value of transmission coefficient (2.23×10^{-3}), while the lowest value of the transmission (1.61×10^{-4}) is presented by molecule R-1. The order of the transmission is $T(E)R-5 > T(E)R-4 > T(E)R-3 > T(E)R-2 > T(E)R-1$. These outcomes could be explained in terms of the increasing of the donor atoms (oxygen atoms) at the wheels. That means is the raising of oxygen atoms from 3 atoms for R-1 to 15 atoms for R-5, leads to a significant raising in the transferred electrons Γ as shown in Figure 4, which leads to increase the value of transmission coefficient. Furthermore, the rings can act as additional pathways for electrons to pass through the molecule, providing more channels for conduction. What is more, the rings can also affect the geometry and orientation of the molecule, which can influence the overlap between the molecular orbitals involved in electron transport. As a result, the electronic coupling between the rings and the rest of the molecule can increase, leading to a higher transmission coefficient.

On the other hand, it can be seen that the transport mechanism for molecules are a LUMO-dominated transport, and this ascribed to type of anchor groups, which is the pyridine anchor group. This result is consistent with previous studies [18, 19].

Table 1 shows that the number of transferred electrons is 196.6 for molecule R-1, which is the lowest value. Whereas, the highest value is 542 electrons for molecule R-5. In contrary, the table shows that the highest H-L gap is -1.14 eV for molecule R-1, while the lowest once is -1.05 eV for molecule R-5. These results predicate an important relationship between Γ , $T(E)$, and H-L gap, since the increasing of Γ results in a high $T(E)$, and low H-L gap, and vice-versa. These results as mentioned previously is ascribed to the quantum size effect phenomenon.

3.2.2 Binding energy (B.E.)

The binding energy (B.E.) is the lowest energy required to make the system stable at an "equilibrium interaction distance". The binding energies between anchor groups and

gold electrodes for the optimized configurations have been calculated. It is well known that SIESTA employs a localized basis set and therefore these calculations are subject to errors. Consequently, the counterpoise method has been used to obtain accurate energies [20]. This involves calculating the total DFT energies for the system (Molecule plus gold (EMG)). The molecule alone (EM), but with the same conformation adopted in the presence of gold electrode and in the absence of the molecule (EG). With these data the binding energies BE have been calculated according to the expression as shown in Equation (1) [21].

$$BE = E_{MG} - E_M - E_G \quad (1)$$

In this study the binding energy refers to the strength of the intermolecular interactions between the wheels and the axle that hold the molecule together, and therefore Equation (1) could be written as:

$$BE = E_{AB} - E_A - E_B \quad (2)$$

where E_{AB} is the total energy of the system involves wheels and the axle. E_A is the total energy of the system but with

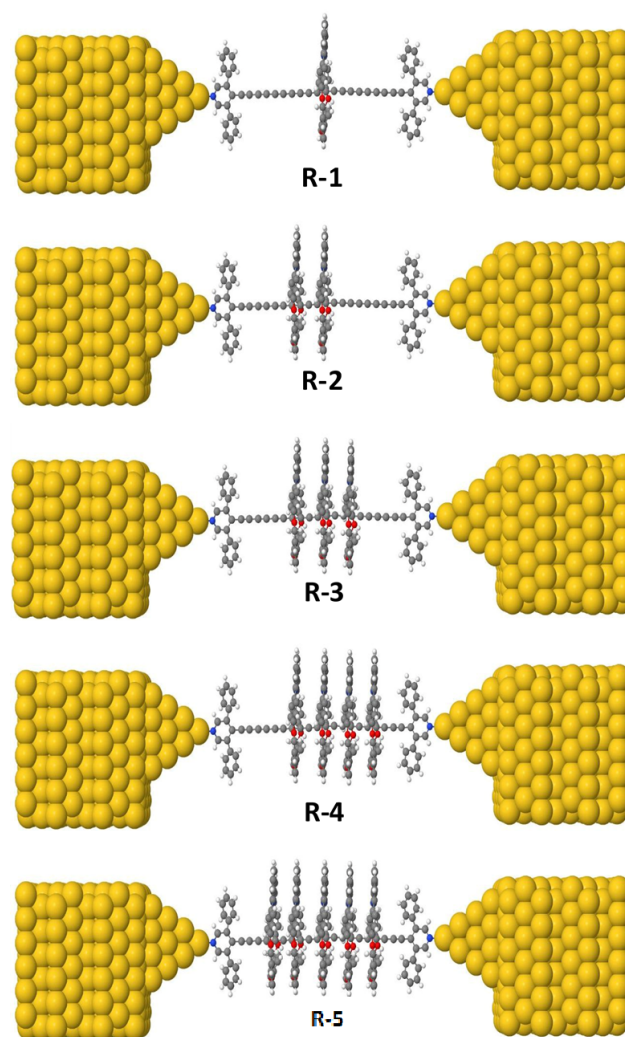


Figure 3. The optimized geometries at ground state of all molecular junctions.

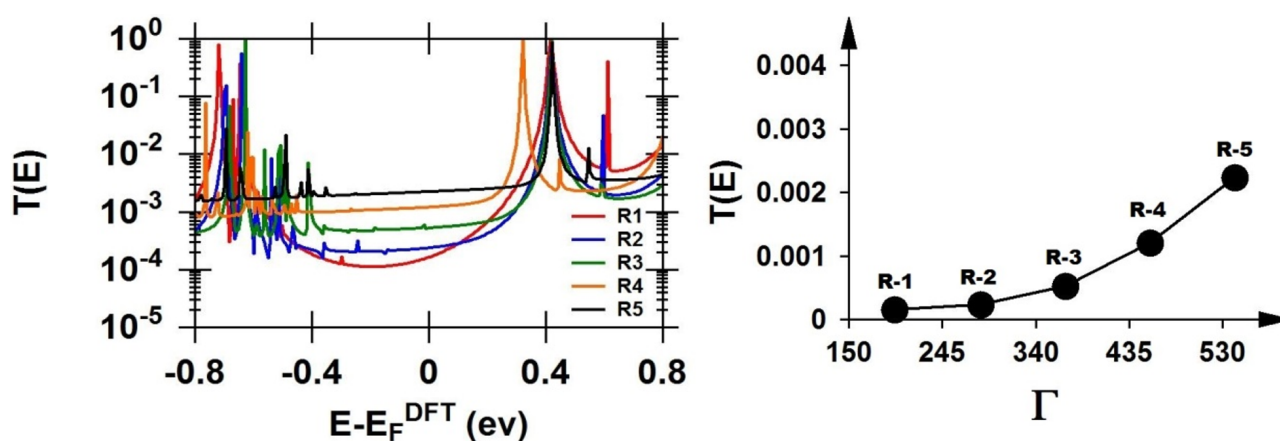


Figure 4. Represents the transmission coefficient $T(E)$ as a function of electrons energy and as a function of the number of electrons transferred from molecule to electrodes of all molecular junctions of all molecules.

the same conformation adopted in the presence of axel, while E_B is the total energy of the system in the absence of the axel.

Figure 5 predicates that the value of binding energy of rotaxane molecules has been fluctuated from -0.46 eV for R-1, then it decreased to -0.25 eV for R-2. Sharply, it raised to -0.61 eV for R-3, and again it lowered to -0.32 eV for R-4. Dramatically, the binding energy increased to the highest value -0.72 eV for R-5. These results reflect an important result to design the rotaxane molecule for drug delivery applications, since the rotaxane molecule with odd numbers of wheels leads to the highest values of binding energies, thus the mechanical bond function of this molecule is exploited through the results that appeared for the binding energy and utilizing the unique properties of the mechanical bond to construct functional systems for medical applications for drug delivery and this feature is main character for this kind of applications.

3.3 Electric and thermoelectric characteristics

3.3.1 Electrical conductance (G/G_0)

Figure 6 shows that the highest electrical conductance is presented by R-5, while the lowest once is introduced via R-1, as well as the conductance raise with increasing the number of wheels in rotaxane molecule. These results could be interpreted in terms of the band theory of solids, since

the increasing of number of wheels results in increasing in the electronic density of states at the Fermi level, which increases the intensity of LUMO resonance peaks as shown in Figure 6, which increases the conductance. In addition, the existence of multi-wheels in rotaxane molecule drives to an important impact of the electric field on the charges distribution and the energy levels of the molecular orbitals, leading to an increase in conductance.

Table 2 and Figure 4 illustrate an important result, which is the electrons transport mechanism, since the theoretical Fermi energy (0.0 eV) is located at the middle of the HOMO-LUMO gap close to the LUMO peak resonance. In addition, the intensity of LUMO peaks is higher than that of the HOMO peaks, the transport mechanism is a HOMO-dominated transport.

3.3.2 Thermo power (S) and figure of merit (ZT_e)

The thermopower, also known as Seebeck coefficient, of a rotaxane molecule describes the magnitude and sign of the voltage generated across the molecule in response to a temperature gradient. The thermopower is a measure of the ability of the molecule to convert a temperature difference into an electrical signal, and is an important parameter for the development of thermoelectric materials and devices [22].

Thermopower is one of the most important properties for the

Table 1. Shows the energy levels HOMOs (the highest occupied molecular orbital), and LUMOs (the lowest unoccupied molecular orbital). $T(E)$ is the transmission coefficient. Γ is the number of electrons transferred from molecules to electrodes. H-L gap is the energy gap between the HOMO and LUMO.

Molecule	$T(E)$	Γ	HOMO (eV)	LUMO (eV)	H-L gap (eV)
R-1	1.6×10^{-4}	196.6	-0.72	0.42	-1.14
R-2	2.4×10^{-4}	283.8	-0.69	0.42	-1.11
R-3	5.2×10^{-4}	369.9	-0.67	0.42	-1.09
R-4	1.2×10^{-3}	455.9	-0.76	0.31	-1.07
R-5	2.3×10^{-3}	542.0	-0.63	0.42	-1.05

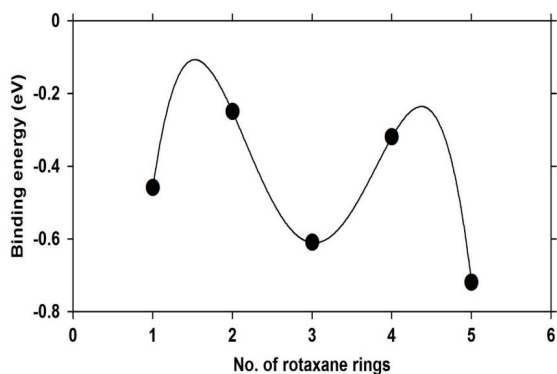


Figure 5. The three-dimensional layout of athermalized fisheye system in the temperature range of Iran.

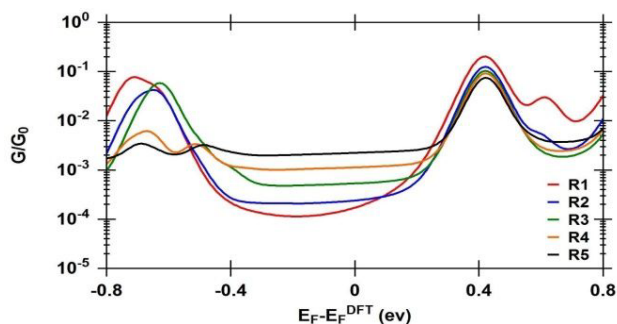


Figure 6. The three-dimensional layout of athermalized fisheye system in the temperature range of Iran.

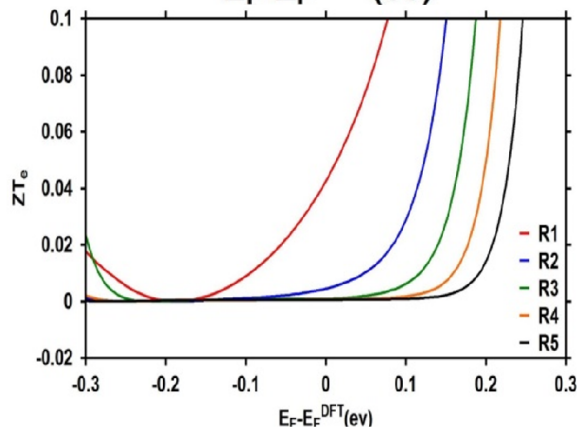
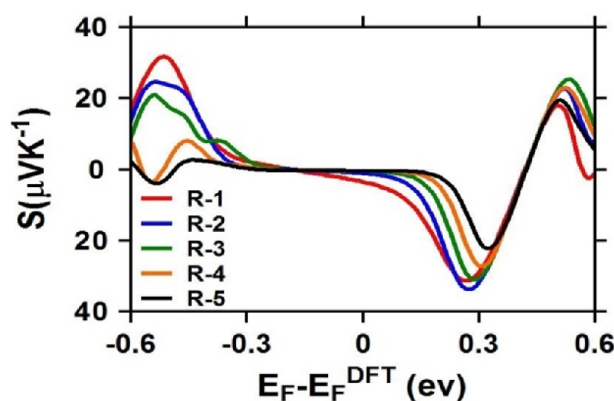


Figure 7. The three-dimensional layout of athermalized fisheye system in the temperature range of Iran.

thermoelectric applications. Figure 7 shows one of the most remarkable results of this work, which is the sign of the thermopower is negative, and that consistent with previous results that the transport mechanism is LUMO-dominated transport. These results also demonstrated that there is a strong relation between the thermopower and electrical conductance, since the high thermopower $-29 \mu\text{VK}^{-1}$ for molecule R-1 yields the lowest conductance as shown in Figure 7 and Table 3, whereas the low thermopower $-19 \mu\text{VK}^{-1}$ for molecule R-5 gives the highest conductance. On the other hand, it could be observed that the thermopower value is very sensitive to the position of the Fermi energy. This could be attributed to the delocalization of the electrons, leading to a higher degree of electronic mobility and a lower resistance to the flow of charge carriers, and that

consequently leads to increase or lower the thermopower values.

Figure of merit (ZT_e) is a metric used to evaluate the performance of a material for a specific application. In the case of a rotaxane molecule, the ZT_e would depend on the application of interest. For example, if the rotaxane molecule is being considered for use in a thermoelectric device, the ZT_e might be defined as the ratio of the electrical conductivity to the thermal conductivity multiplied by the Seebeck coefficient. In terms of low electrical conductance yields high thermopower, the results presented in Table 3 show that the lowest conductance is introduced by R-1, which leads to a significant raising of electronic figure of merit value 0.05, and the highest value of Seebeck coefficient, while the highest conductance of molecule R-5 results in the lowest value

Table 2. Shows the electrical conductance (G/G_0). H_{PI} is the HOMO resonance peak intensity. L_{PI} is the LUMO peak resonance intensity. V_{th} is the threshold voltage.

Molecule	(G/G_0)	H_{PI} (eV)	L_{PI} (eV)	V_{th} (eV)
R-1	1.5×10^{-4}	7.6×10^{-2}	2×10^{-1}	0.47
R-2	2.3×10^{-4}	5.9×10^{-2}	1.3×10^{-1}	0.45
R-3	5.1×10^{-4}	4.3×10^{-2}	1×10^{-1}	0.44
R-4	1.1×10^{-3}	6.1×10^{-3}	9.2×10^{-2}	0.43
R-5	2.2×10^{-3}	3.4×10^{-3}	7.5×10^{-2}	0.42

Table 3. Shows electrical conductance, thermopower (S) and electronic figure of merit (ZT_e).

Molecule	(G/G ₀)	S μ VK ⁻¹	ZT_e
R-1	1.5×10^{-4}	-29	0.05
R-2	2.3×10^{-4}	-24	0.01
R-3	5.1×10^{-4}	-22	0.009
R-4	1.1×10^{-3}	-20	0.007
R-5	2.2×10^{-3}	-19	0.006

0.006 of ZT_e . In general, the values of the electronic figure of merit are low, and it is clear there is a strong connection between electrical conductance, thermopower and figure of merit which definitely needs more investigations. However, these results predicated that the changing of number of rotenone wheels could be a promise strategy to influence, control and may be enhance the thermoelectric properties of this kind of molecular junctions.

4. Conclusion

In conclusion, the results show that the structural and morphological characteristics such as the size, shape and number of axle and macrocycle wheels in rotaxane molecule are important parameters that determine not only the structural aspects but also the electronic and thermoelectric properties. The transmission coefficient values were high and this an evidence of the constructive interference, which has been controlled and enhanced via changing the number of wheels in rotaxane molecules. In addition, the increasing of wheels' number impacted the HOMO-LUMO gap, and this contributed in raising or lowering the transmission coefficient values. A remarkable conclusion introduce itself from this work, which is the strong relationship between electrical conductance, thermopower and figure of merit which definitely needs more investigations. In general, the highest conductance yields to low thermopower and figure of merit. All concluded introduce a strong suggestion that the molecular junctions based on rotaxane molecules are promising candidates for electronic and thermoelectric applications. A conclusion could be drawn from this work that the rotaxane molecules with odd numbers of wheels leads to the highest values of binding energies. This result proposes robustly that the rotaxane molecules are vigorous candidates for drug delivery applications.

Authors Contributions

Hiba Abbas Mohammed write the main text, simulate and finalized it, Oday A. Al-Owaedi and Hussein Neama Najeeb supervised and advised the work and also edit the text.

Availability of Data and Materials

The data that support the findings of this study are available from the corresponding author upon reasonable request.

Conflict of Interests

The authors declare that they have no known competing financial interests or personal relationships that could have appeared to influence the work reported in this paper.

Open Access

This article is licensed under a Creative Commons Attribution 4.0 International License, which permits use, sharing, adaptation, distribution and reproduction in any medium or format, as long as you give appropriate credit to the original author(s) and the source, provide a link to the Creative Commons license, and indicate if changes were made. The images or other third party material in this article are included in the article's Creative Commons license, unless indicated otherwise in a credit line to the material. If material is not included in the article's Creative Commons license and your intended use is not permitted by statutory regulation or exceeds the permitted use, you will need to obtain permission directly from the OICC Press publisher. To view a copy of this license, visit <https://creativecommons.org/licenses/by/4.0>.

References

- [1] G. E. Moore. "Cramming more components onto integrated circuits.". *Electronics*, **38**:8, 1965. DOI: <https://doi.org/10.1109/N-SSC.2006.4785860>.
- [2] J. M. Tour. "Molecular electronics: Synthesis and testing of components.". *Accounts of Chemical Research*, **33**:791–804, 2020. DOI: <https://doi.org/10.1021/ar0000612>.
- [3] J. C. Cuevas and E. Scheer. "Molecular electronics: An introduction to theory and experiment.". *World Scientific Series in Nanoscience and Nanotechnology*, **1**:724, 2010.
- [4] C. J. Bruns and J. F. Stoddart. "Rotaxane-based molecular muscles.". *Accounts of Chemical Research*, **47**:2186–2199, 2014. DOI: <https://doi.org/10.1021/ar500138u>.
- [5] K. E. Drexler. "Nanosystems: molecular machinery, manufacturing, and computation.". *John Wiley & Sons*, , 1992.
- [6] A. Rao and H. Cölfen. "Comprehensive supramolecular chemistry II: Facet control in nanocrystal growth.". *Book: Comprehensive Supramolecular Chemistry II*, : 129–156, 2017. DOI: <https://doi.org/10.1016/B978-0-12-409547-2.12638-1>.

- [7] B. Xu and N. J. Tao. “Measurement of single-molecule resistance by repeated formation of molecular junctions.”. *Science*, **301**:1221–1223, 2003. DOI: <https://doi.org/10.1126/science.1087481>.
- [8] N. Argaman and G. Makov. “Density functional theory: An introduction.”. *American Journal of Physics*, **68**:69–79, 2000. DOI: <https://doi.org/10.1119/1.19375>.
- [9] W. Kohn, A. D. Becke, and R. G. Parr. “Density functional theory of electronic structure.”. *Journal of Physical Chemistry*, **100**:12974–12980, 1996. DOI: <https://doi.org/10.1021/jp960669l>.
- [10] T. Van Mourik and R. J. Gdanitz. “A critical note on density functional theory studies on rare-gas dimers.”. *Journal of Chemical Physics*, **116**:9620–9623, 2002. DOI: <https://doi.org/10.1063/1.1476010>.
- [11] J. E. M. Soler, E. Artacho, J. D. Gale, A. García, J. Junquera, P. Ordejón, and D. Sánchez-Portal. “The SIESTA method for ab initio order-N materials simulation.”. *Journal of Physics: Condensed Matter*, **14**:2745–2779, 2002. DOI: <https://doi.org/10.1088/0953-8984/14/11/302>.
- [12] E. Artacho, E. Anglada, O. Dieguez, J. D. Gale, A. Garcia, J. Junquera, R. M. Martin, P. Ordejón, J. M. Pruneda, D. Sanchez-Portal, and J. M. Soler. “The SIESTA method; Developments and applicability.”. *Journal of Physics: Condensed Matter*, **20**:064208, 2008. DOI: <https://doi.org/10.1088/0953-8984/20/6/064208>.
- [13] J. Ferrer, C. J. Lambert, R. J. Bushby, and M. R. Bryce. “GOLLUM: a next-generation simulation tool for electron, thermal and spin transport.”. *New Journal of Physics*, **16**:093029, 2014. DOI: <https://doi.org/10.1088/1367-2630/16/9/093029>.
- [14] J. A. Bravo, F. M. Raymo, J. F. Stoddart, A. J. P. White, and D. Williams. “High yielding template-directed syntheses of [2] rotaxanes.”. *European Journal of Organic Chemistry*, **1998**, 1998. DOI: [https://doi.org/10.1002/\(SICI\)1099-0690\(199811\)1998:11<2565::AID-EJOC2565>3.0.CO;2-8](https://doi.org/10.1002/(SICI)1099-0690(199811)1998:11<2565::AID-EJOC2565>3.0.CO;2-8).
- [15] J. S. Meisner, S. Ahn, S. V. Aradhya, M. Krikorian, R. Parameswaran, M. Steigerwald, and C. Nuckolls. “Importance of direct metal- π coupling in electronic transport through conjugated single-molecule junctions.”. *Journal of the American Chemical Society*, **134**:20440–20445, 2012. DOI: <https://doi.org/10.1021/ja308626m>.
- [16] J. Xia, B. Capozzi, S. Wei, M. Strange, A. Batra, J. R. Moreno, and L. M. Campos. “Breakdown of interference rules in azulene, a no alternant hydrocarbon.”. *Nano Letters*, **14**:2941–2945, 2014. DOI: <https://doi.org/10.1021/nl5010702>.
- [17] D. J. Griffiths. “Introduction to quantum mechanics. 2nd edition.”. *Pearson Prentice Hall*, , 2004. DOI: <https://doi.org/10.30495/JOPN.2024.31998.1291>.
- [18] H. Vazquez, R. Skouta, S. Schneebeli, M. Kamenetska, R. Breslow, L. Venkataraman, and M. S. Hybertsen. “Probing the conductance superposition law in single-molecule circuits with parallel paths.”. *Nature Nanotechnology*, **7**:663–667, 2012. DOI: <https://doi.org/10.1038/nnano.2012.147>.
- [19] S. F. Boys and F. J. M. P. Bernardi. “The calculation of small molecular interactions by the differences of separate total energies. Some procedures with reduced errors.”. *Molecular Physics*, **19**:553–566, 1970. DOI: <https://doi.org/10.1080/00268977000101561>.
- [20] H. Ozawa, M. Baghernejad, O. A. Al-Owaedi, V. Kaliginedi, T. Nagashima, J. Ferrer, and M. A. Haga. “Synthesis and single-molecule conductance study of redox-active ruthenium complexes with pyridine and dihydrobenzo[b]thiophene anchoring groups.”. *Chemistry - A European Journal*, **22**:12732–2740, 2016. DOI: <https://doi.org/10.1002/chem.201600616>.
- [21] H. Jansen and P. Ros. “Non-empirical molecular orbital calculations on the protonation of carbon monoxide.”. *Chemical Physics Letters*, **3**:140–143, 1969. DOI: [https://doi.org/10.1016/0009-2614\(69\)80118-1](https://doi.org/10.1016/0009-2614(69)80118-1).
- [22] A. C. Olivier and G. M. Escandar. “Analytical figures of merit.”. *Book: Practical Three-Way Calibration*, **21**:778–788, 2014.